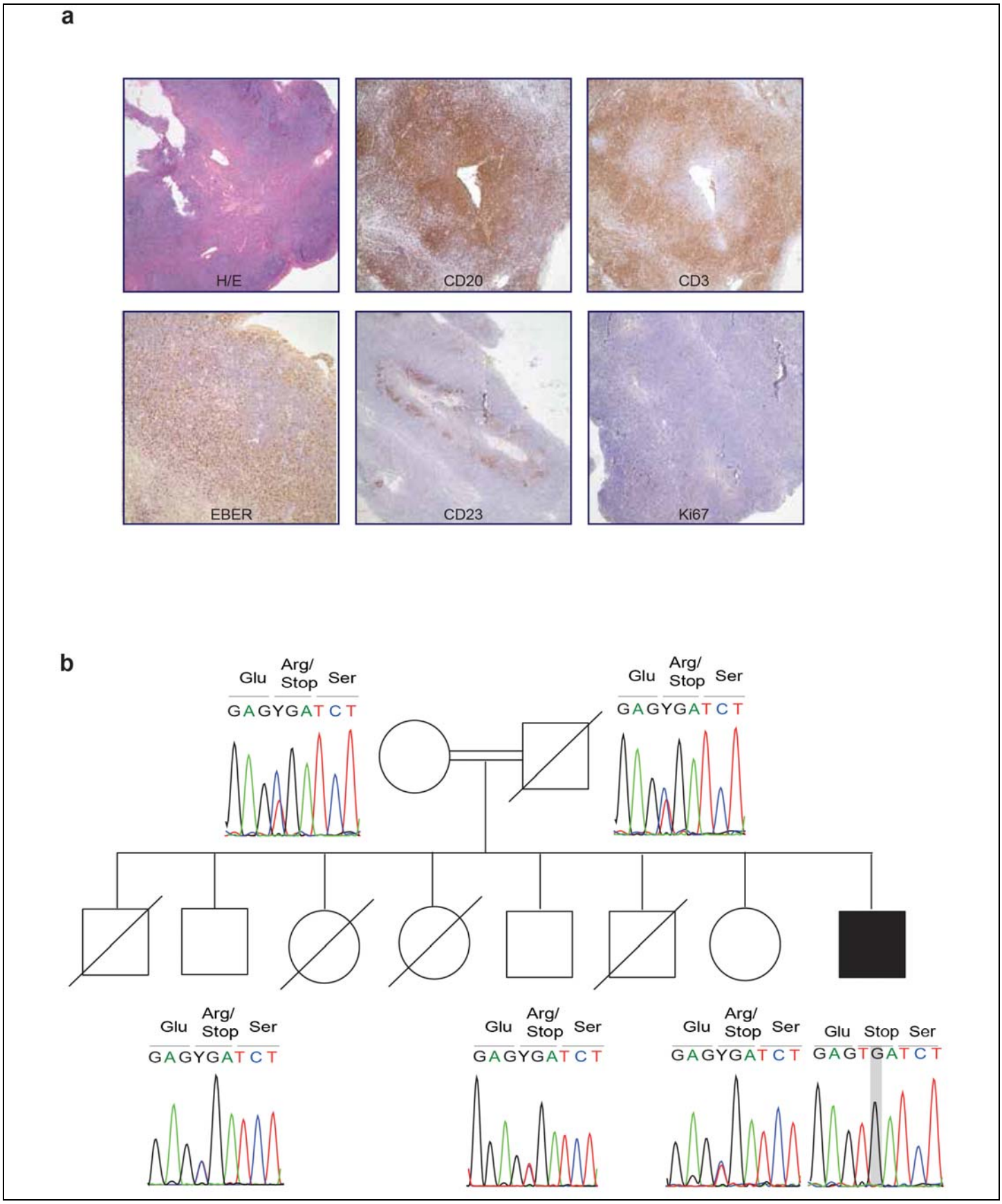
a
H/E
CD20
CD3
EBER
CD23
Ki67
b
Glu
Arg/
Stop
Ser
GAGYGATCT
Glu
Arg/
Stop
Ser
GAGYGATCT
Glu
Arg/
Stop
Ser
GAGYGATCT
Glu
Arg/
Stop
Ser
GAGYGATCT
Glu
Stop
Ser
GAGTGATCT

Supplementary Figure 1
Histology of lymphoma and segregation of the mutation with the disease phenotype.
(a) Histology of adenoid biopsy showing low grade B-cell lymphoma compatible with marginal zone lymphoma. Top left to right: Hematoxilin/Eosin staining, CD20 staining, CD3 staining. Bottom left to right: EBER, CD23, Ki67. The described findings suggest a low grade EBV-related B-cell lymphoma developed likely associated with the underlying immunodeficiency. (b) Segregation of the detected mutation among the core family (circle - female; square - male; line - dead; black filling - affected index patient).

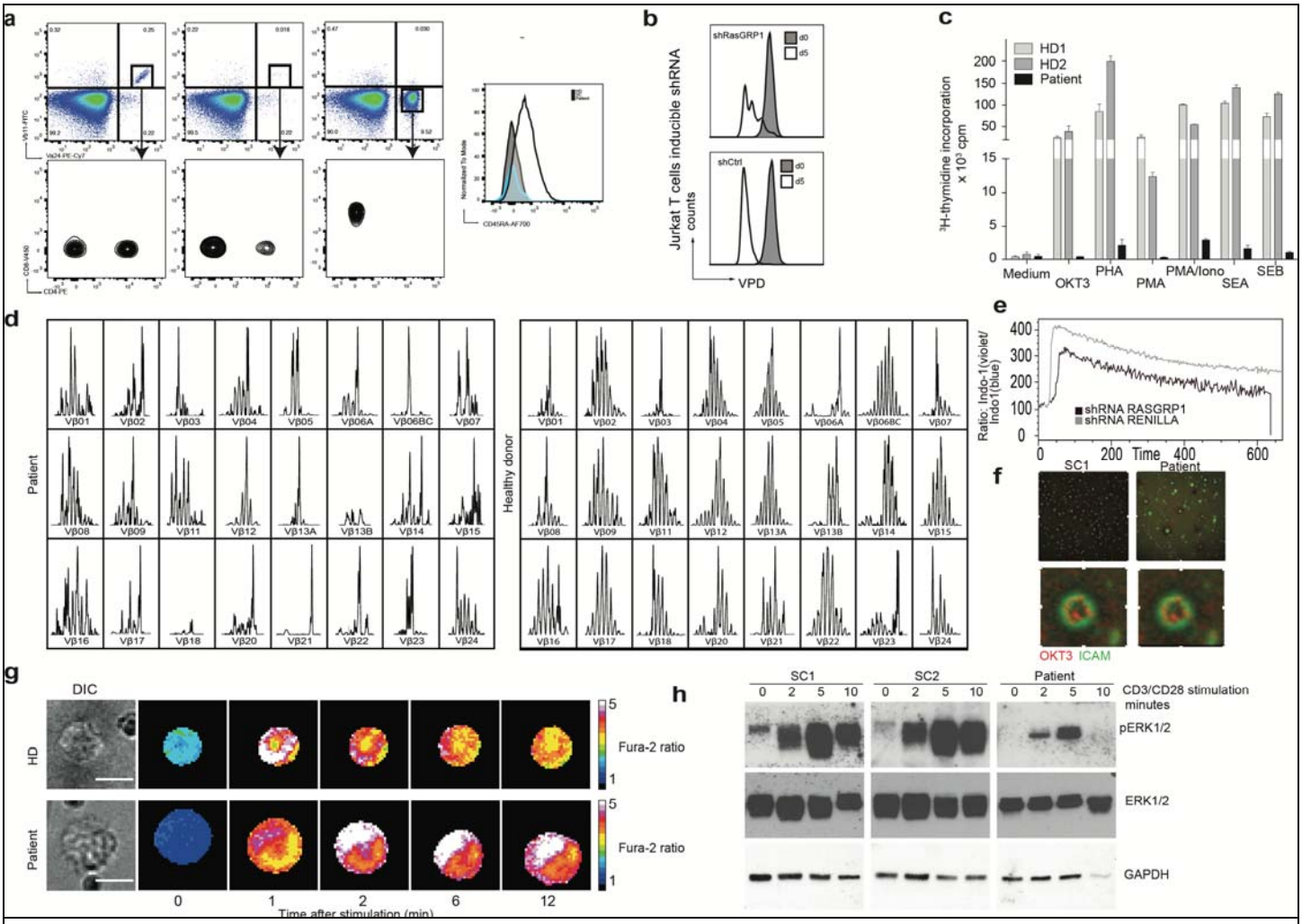

Supplementary Figure 2

Functional characterization of T cells.

(a) Invariant natural killer T (iNKT) cells. A prominent TCRvα24-expressing cell population was detectable in patient peripheral blood, however these cells expressed CD8 and CD45RA surface markers, suggesting that they belong to oligoclonally expanded exhausted memory CD8 T cells. HD – healthy donor; SC – Shipment control. (b) Proliferative response of T cells determined by [^{3}H]-thymidine incorporation assay after stimulation with various stimuli after 3 days (OKT3, anti-CD3 antibody (clone OKT3)); PMA, phorbol 12-myristate 13-acetate; SEA: Staphylococcal enterotoxin A; SEB: Staphylococcal enterotoxin B; PHA: phytohaemagglutinin). (c) Proliferation of Jurkat T cells upon shRNA-mediated knockdown of *RASGRP1*. shRNA against Renilla luciferase was used as negative control. Cells were labeled with violet proliferation dye and analyzed by flow cytometry over the period of 5 days. (d) TCRVβ spectratyping of patient and control T cells indicating oligoclonality of the TCR repertoire of the patient. (e) Calcium flux of Jurkat T cells upon inducible shRNA-mediated knockdown of *RASGRP-1*. shRNA against Renilla luciferase was used as negative control. (f) Fluorescence microscopy of Ca^{2+}-flux of one representative cell is displayed below the graph. Scale bar represents 10 µm. HD–healthy donor; DIC–differential interference contrast. (g) ICAM Ring formation and cSMAC exclusion of hTERT immortalized patient and control T cell lines on a lipid bilayer following OKT3 stimulation. (h) Cropped immunoblot showing downstream TCR signaling in expanded patient and shipment T cells upon CD3/CD28 stimulation. Cells were starved and restimulated with anti-CD3/anti-CD28 antibodies and subsequently analyzed for ERK1/2 phosphorylation. Data is representative of three (h), two (a,c,d,g) or one (b,f,e) independent experiment.

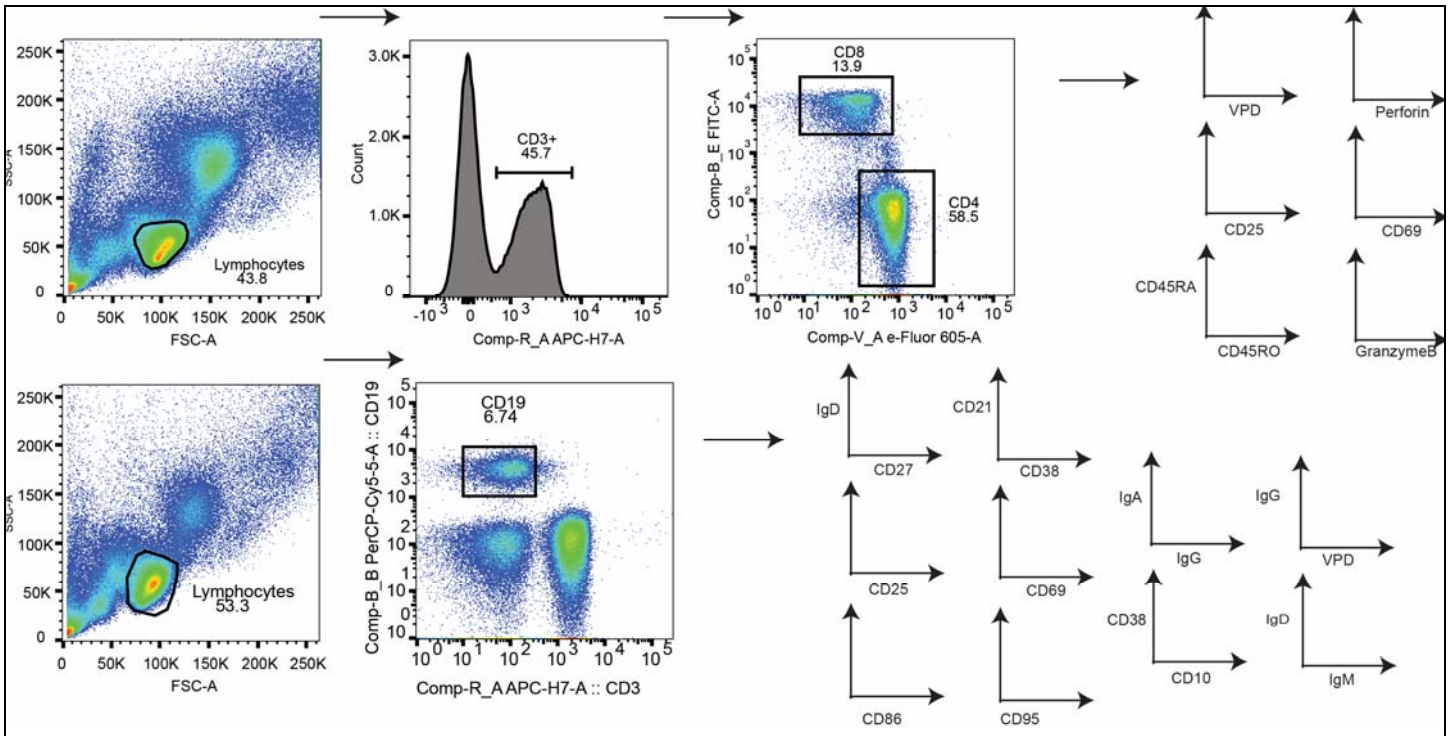

Supplementary Figure 3

Gating Strategy

Gating strategy for Figures 2 and 3 are presented in this figure.a

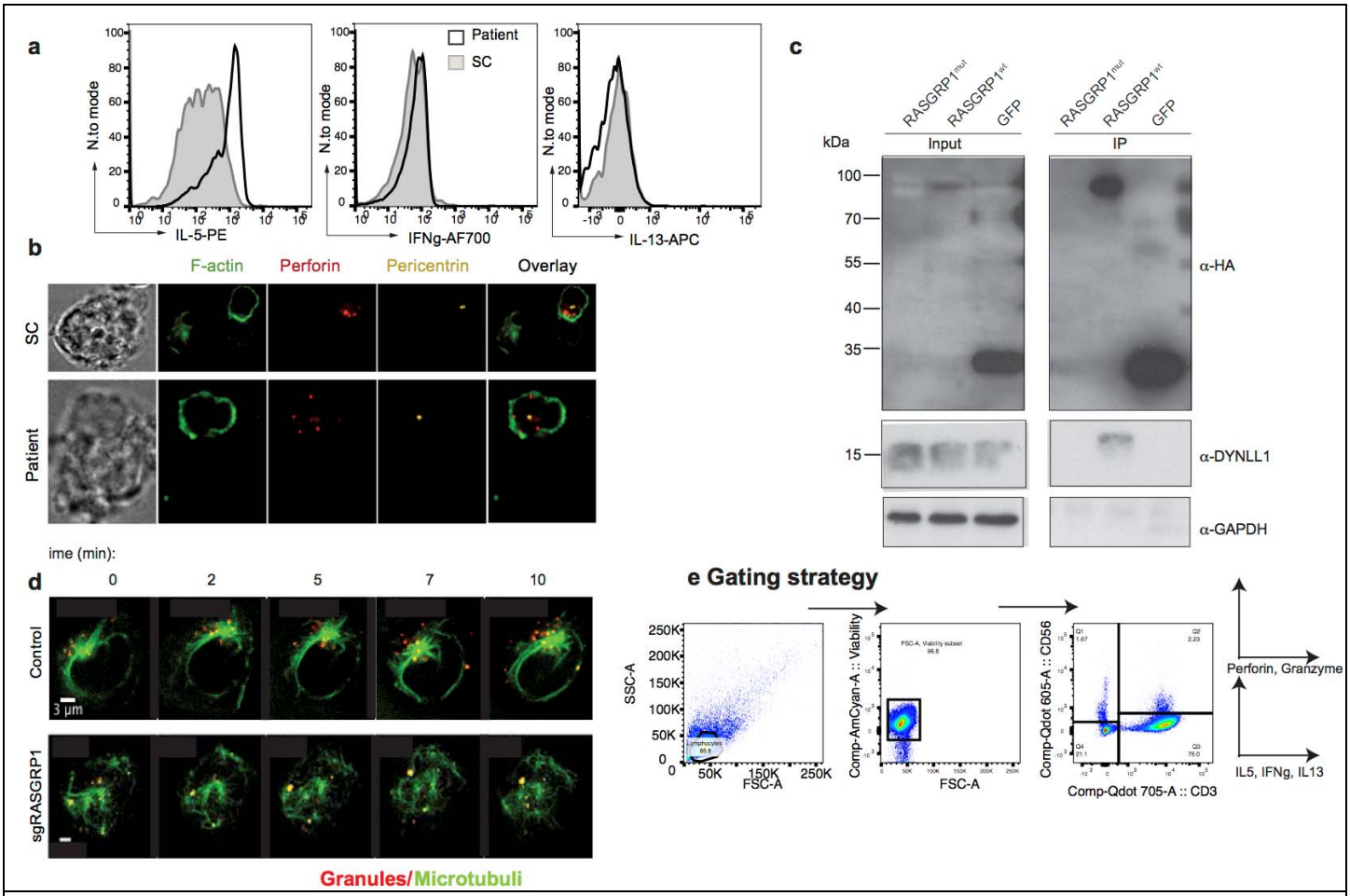

Supplementary Figure 4

NK-cell studies.

(a) Flow cytometric analysis of intracellular accumulation of IL-5, IL13 and IFNγ in patient and control NK cells. (b) Immune synapse formation in primary patient NK cells (c) Co-immunoprecipitation of Strep-HA tagged RASGRP1 with endogenous dynein light chain 1 (DYNLL1) (RASGRP1wt) wildtype Strep-HA-tagged RASGRP1 and (RASGRP1mut) mutant Strep-HA-tagged RASGRP1. Strep-HA-tagged GFP was used as negative control. (d) Video microscopy of granule convergence in CRISPR-edited NK-92 cells lines HD, healthy donor. (d) Video microscopy of control or sgRASGRP1 NK-92 cells for granule convergence (Granules-red, Microtubuli-green). Data are representative of two biological replicates (a-d).(e) Gating strategy of FACS plots in Figure 4.

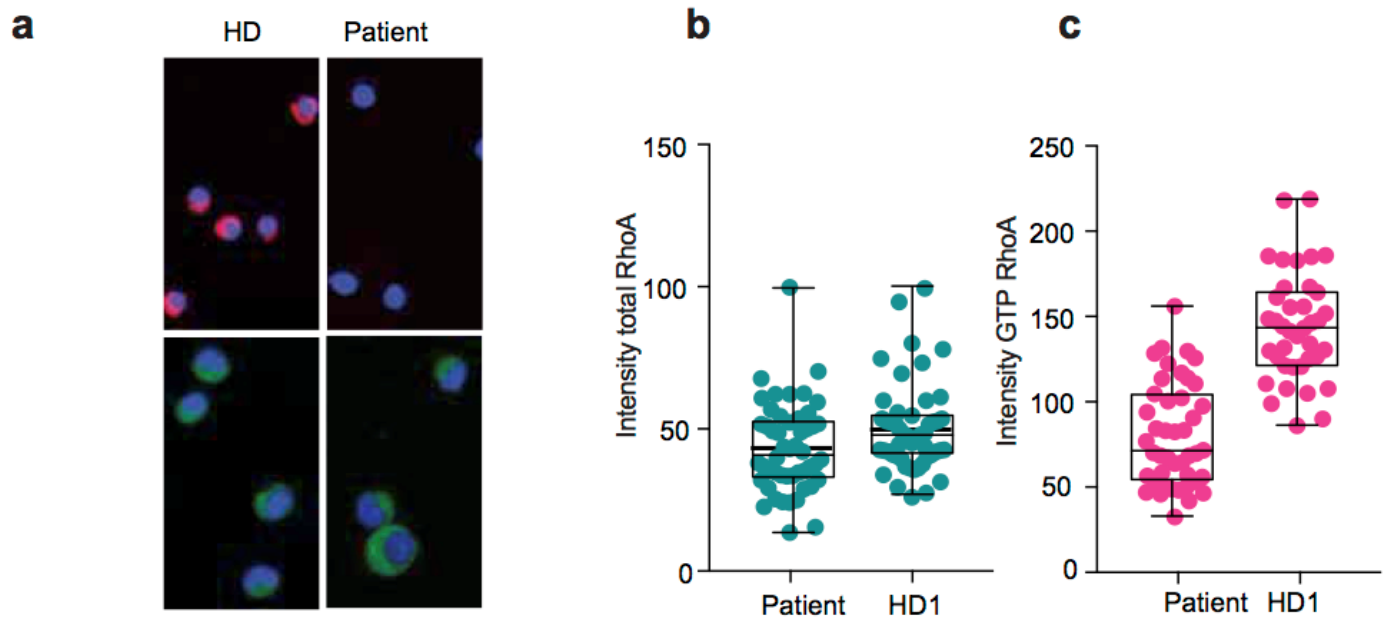

Supplementary Figure 5

T-cell activation using CXCL12.

(a-c) Immunofluorescence (a) and quantification (b,c) of patient and healthy donor expanded CD8 T cells following CXCL12 stimulation either stained for total RhoA (green) or active RhoA (pink) and DAPI (blue). Data is representative of two (a-c) independent experiments.